Mon. Not. R. astr. Soc. (1990) **245**, 749–758

The stellar population and emitting gas in the inner 2–5 kpc for a sample of nine Seyfert 2 galaxies

T. Storchi Bergmann,* E. Bica and M. G. Pastoriza*
Instituto de Fisica, Universidade Federal do Rio Grande do Sul, CP 15051, Porto Alegre, RS, Brasil

Accepted 1990 March 19. received 1990 March 16; in original form 1989 December 5

SUMMARY

We analyse the stellar population and the emitting gas in the inner 2–5 kpc of a sample of nine Seyfert 2 galaxies, using 5-Å resolution spectra in the range 3600–7000 Å. The typical population is old and moderately stronglined, except in IC 5135 which presents star-forming events. The emission-line spectrum is studied after subtraction of the stellar population. Broad Hα components (FWHM = 2000 km s^{-1}) were found for five of the galaxies. The line widths correlate with the critical densities for the forbidden lines in four of the galaxies and with the ionization potential in three of these, indicating the presence of density stratification and ionization structure. Comparison of our emission-line ratios with smaller aperture data obtained from the literature reveal important changes in the values due to contamination by surrounding gas. Using photo-ionization models we derive gas abundances between solar and two-times solar, with an overabundance of nitrogen in NGC 4939 and 6890, and of nitrogen and sulphur in NGC 1667, relative to the other heavy elements.

1 INTRODUCTION

The emphasis in spectral studies of Seyfert 2 galaxies has been mostly focused on the emission-line spectra of the nuclei, measured with apertures of 2 arcsec (e.g. Koski 1978; Phillips, Charles & Baldwin 1983). However, it is also important to analyse the global spectra of the central regions, including the underlying and the surrounding stellar populations and emitting gas. Indeed, in the neighbourhood of active nuclei, interesting phenomena occur, like extended gas emission and enhanced star formation, as well as the eventual appearance of structures like rings and jets (Sersic & Pastoriza 1967; Osmer, Smith & Weedman 1974; Baldwin, Wilson & Whittle 1987; Colina *et al.* 1987; Durret & Bergeron 1988).

The aim of this work is to study the relative importance of the various stellar components and the emitting gas seen globally through apertures of 5–8 arcsec in nearby galaxies, corresponding in our sample to the central 2–5 kpc. This kind of study is important in order to reproduce the observational conditions of more distant galaxies, for which the spatial resolution is small even for narrow apertures. We investigate correlations between line width of emission lines and critical density, and between line width and ionization potential (Pelat, Alloin & Fosbury 1981; Filippenko 1985; de Robertis & Osterbrock 1984, 1986). We also investigate the presence of Hα broad components. From the relative intensities of the emission lines, we derive temperature and density of the emitting gas, as well as the slope of the ionizing continuum and an estimate of the metal abundance by comparison with theoretical ratios obtained from photo-ionization models.

2 OBSERVATIONS

We have observed the galaxies with the 1-m telescope of Cerro Tololo Inter-American Observatory using the cassegrain spectrograph and the 2D-FRUTTI two-dimensional photon-counting detector. All the spectra were flux calibrated, and cover the range 3600–7000 Å, with a spectral resolution of 5 Å at 5000 Å (FWHM of comparison lamp lines). NGC 1667, 6890, IC 5063 and 5135 were observed in 1986 September using a slit width of 8 arcsec. NGC 3281, 4939 and 4507 were observed in 1987 March, and NGC 2992 and 4388 in 1988 May, with a slit width of 5 arcsec. The final spectra are the sum of the light detected in six pixels (11 arcsec) along the slit, centred on the nucleus.

Table 1 lists the morphological types and absolute magnitudes (Sandage & Tammann 1981) as well as the dimensions in kiloparsecs corresponding to the extracted spectra, adopting $H_0 = 50$ km s^{-1} Mpc^{-1}. The observed radial velocity, which we measured from [O III] λ5007, is given in column 5. For most of the galaxies these values do not differ by more

*Visiting observers, Cerro Tololo Inter-American Observatory, National Optical Astronomy Observatories.

Table 1. Basic data.

Galaxy	Morphol.	M_B	Slit(Kpc)	V_R(Km/s)	E(B-V)$_G$	E(B-V)$_\perp$	E(B-V)$_\parallel$
1)N1667	Sc(r):IIpec	-22.54	4.8x3.5	4540	0.04	0.01	0.63
2)N2992	Sa(tides)	-21.36	2.3x1.1	2390	0.03	0.35	0.07
3)N3281	Sa	-22.11	3.8x1.7	3400	0.07	0.25	0.83
4)N4388	Sab	-21.05	2.7x1.2	2520	0.00	0.38	0.38
5)N4507	SBab(rs)I	-21.96	3.7x1.7	3390	0.05	0.10	0.10
6)N4939	Sbc(rs)I	-22.77	3.3x1.5	3000	0.00	0.10	0.26
7)N6890	Sab(s)II-III	-21.06	2.6x1.9	2490	0.03	0.03	0.45
8)I5063	SO_a(3)pec/Sa	-20.95	3.6x2.6	3120	0.02	0.15	0.13
9)I5135	Sa pec	-22.27	5.1x3.7	4800	0.00	0.00	0.32

than 100 km s^{-1} from the value in Sandage & Tammann (1981), except in the cases of NGC 2992, 3281 and IC 5063. Nevertheless, more recent data agree with our values for NGC 2992 (Colina *et al.* 1987) and NGC 3281 (Durret & Bergeron 1988). In the case of IC 5063, our value is 200 km s^{-1} smaller than that of Bergeron, Durret & Boksenberg (1983). The radial velocity of NGC 4507 is not given by Sandage & Tammann (1981) and our value is 150 km s^{-1} smaller than that of Adney, Wilson & Baldwin (1984). The reddening is listed in the last columns, decomposed in three parts: (1) foreground contribution (Sandage & Tammann 1981); (ii) internal reddening from the population analysis (Section 3); (iii) internal reddening in the line-emitting regions, from the observed flux ratio $F(\mathrm{H}\alpha_{\mathrm{narrow}})/F(\mathrm{H}\beta)$ and assuming a case B recombination value.

In Fig. 1 we show six spectra where the relative emission line intensities can be compared. In Fig. 2 we present the remaining galaxies emphasizing different types of stellar population found in our sample (Section 3).

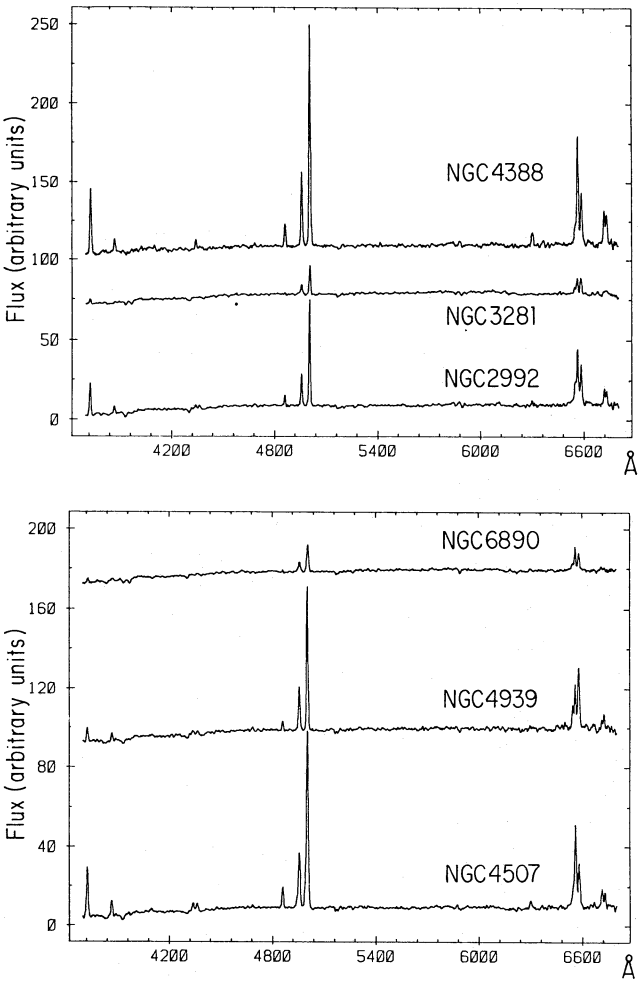

Figure 1. Observed spectra $F(\lambda)$ for six sample galaxies normalized in λ5870 and shifted by arbitrary amounts for clarity.

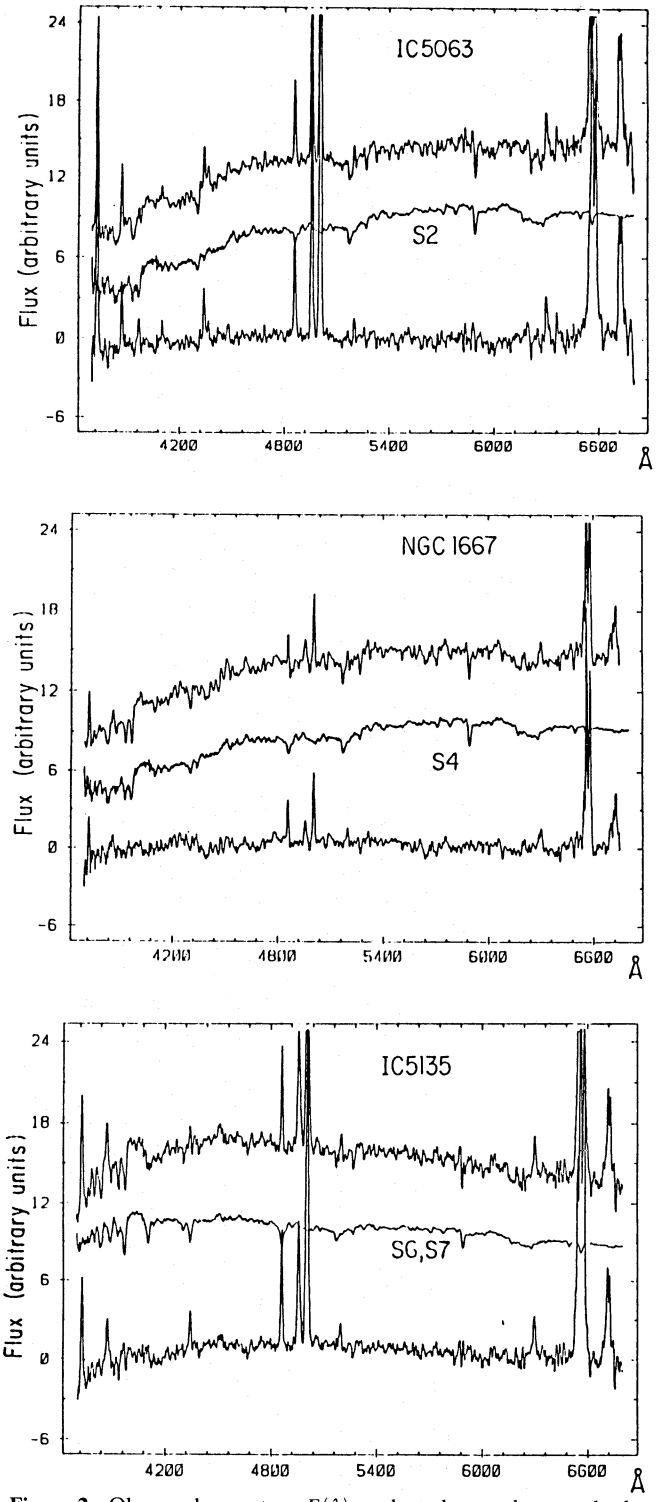

Figure 2. Observed spectra $F(\lambda)$, selected template and the residual, where only the emission component is left for three sample galaxies, showing different kinds of stellar population.

Table 2. Equivalent widths of absorption lines, continuum fluxes and adopted templates.

Galaxy	K(Ca) 3933	Hδ 4102	CN 4200	G 4300	Hγ 4340	Hβ 4861	MgI 5175	NaI 5890	Cont. 4020	Cont. 4570	Temp.
N1667	11.5	5.7	7.4	6.7	6.1	0.6	6.3	4.1	6.3	9.0	S4
N2992	16.9	0.4	4.5	8.0	-0.7	-4.9	7.0	2.7	5.0	7.9	S4
N3281	15.5	2.7	8.9	10.6	6.3	0.5	5.9	3.2	3.7	6.6	S2
N4388	13.4	2.0	12.0	7.8	-1.4	-15.9	6.3	1.9	5.9	7.9	S4
N4507	15.2	-2.8	4.8	6.9	-5.9	-11.0	4.7	3.5	6.3	9.1	S4
N4939	19.1	1.5	10.2	10.0	1.0	-3.3	6.4	3.1	5.1	8.3	S2
N6890	12.6	5.4	8.9	7.4	4.3	1.9	6.2	3.4	5.7	8.3	S3
north[1]	8.8	4.1	3.8	5.5	4.2	1.6	5.3	3.4	7.5	9.7	S5
I5063	14.7	1.7	12.4	8.6	-1.9	-5.5	7.4	5.5	4.5	7.6	S2
I5135	5.8	6.1	7.1	4.1	3.1	-3.1	3.6	3.8	9.0	10.5	S6
north[1]	4.9	5.5	5.6	3.8	4.1	-1.9	5.0	3.1	11.3	11.6	S6,S7[2]

[1]From spectrum centred 5 arcsec north of the nucleus of previous galaxy.
[2]Linear combination of templates: $0.65 \times S6 + 0.35 \times S7$.

3 THE STELLAR POPULATION

The spectra were corrected for foreground reddening from Table 1 and have been rebinned and to the rest frame. We have then analysed the stellar population based on the population-synthetic results of Bica (1988), which describe the stellar content in relation to the properties of star clusters. Table 2 shows the measured equivalent widths (W) of five metallic features and three Balmer lines using the continuum tracing criteria and the window limits as given in Bica (1988) and Bica & Alloin (1986a). We point out that some of these windows are affected by emission, in particular Hβ. Caution is required also for Mg I, owing to the [N I] 5198 Å contamination in the window, and for Na I owing to He I 5876 Å, whose effects were quantified *a posteriori* (after the stellar population template selection as described below). The emission contamination was calculated using observed equivalent widths from Table 2 and template ones from Bica (1988) and Bica & Alloin (1986a). The values $(W_{obs} - W_{templ})/W_{templ} \times 100$ indicate 30 per cent for the strongest contaminations of [N I] in the Mg window. The results for He I in the Na I window are similar, but absorption residuals in some cases also amount to 30 per cent, whereas in the Mg I window they are at most 10 per cent. This is due to the additional contamination of interstellar absorption from the disc in inclined galaxies and also in the nuclear gas (Bica & Alloin 1986b).

Based mainly on the emission-free features W[K(Ca)], W(CN) and W(G) as well as on the continuum distribution, it was possible to find a similar template population in Bica (1988) for the galaxies in our sample. Fig. 2 illustrates the different types of population, together with template subtractions to isolate the pure gas emission. The ratio of residuals-to-template allows us to estimate the percentage deviations from the adopted template. Typically, in 90 per cent of the observed wavelength range, departures do not exceed 10 per cent, although, at the blue end ($\lambda < 3800$ Å), systematic effects due to calibration problems and border effects typically amount to 20 per cent. It is worth noting that these template populations were built from star-cluster spectra and are emission free, and thus particularly suitable for population subtractions. It was also possible to estimate the internal reddening affecting the stellar population using the relations between inclination reddening versus axial ratio b/a for different spiral types (Bica & Alloin 1986a,b); minor extra reddening corrections were necessary in some cases for matching the template to the observed spectrum. We list in column 7 of Table 1 the final internal reddening for the stellar population $E(B-V)_i$.

The templates are listed in Table 2. According to Bica (1988), S2 is the most metallic, attaining $[Z/Z_0] = +0.3$, while the remaining ones have attained solar metallicity. S2 and S3 are red and dominated by the old population, i.e. the strongest flux contribution (~87 per cent at λ5870 Å) comes from components which are globular clusters of different metallicities. In S4 to S6 the contribution of population younger than 10^8 yr increases from 9 to 22 per cent in terms of flux fractions at λ5870 Å.

We conclude (Table 2) that the typical underlying population in our sample of Seyfert 2 galaxies in the central 2–5 kpc is old, and indistinguishable from the usual nuclear population in normal spirals. There is one exception: IC 5135, of type S6 (Fig. 2c), with an important blue component. We do not find evidence of a non-thermal continuum in any of the galaxies in the present spectral range. Even in IC 5135, the bluest nucleus, the blue continuum appears to be of stellar origin, because Balmer absorption lines are clearly present for $\lambda < 3900$ Å, as has been previously noticed by Shields & Filippenko (1988).

For NGC 6890 and IC 5135 we also have at our disposal an off-nuclear spectrum centred at 5 arcsec north, both with H II-region emission. For NGC 6890, this corresponds to a region centred at 1.2 kpc from the nucleus. The respective population is bluer than that of the nucleus (Table 2). For IC 5135, the off-nuclear spectrum is centred at 2.3 kpc north of the nucleus and has practically the same values for the equivalent widths as the nuclear spectrum, but the continuum is somewhat bluer. The meaning of this result is either that the off-nuclear population is bluer than that of the nucleus or that the nucleus has the same population but is reddened. This last hypothesis agrees with observations which indicate that this galaxy has a peculiar central absorption pattern (Dressler & Sandage 1978). We conclude that in these two cases there is star formation in the neighbourhood of the active nucleus, as has been observed, for example, in NGC 1086 (Schild, Tresch-Fienberg & Huchra 1985) and in NGC 7469 (Wilson *et al.* 1986). However, in the case of IC 5135, the star-forming regions reach the nucleus, indicating a widespread burst of star formation in the central regions of this galaxy.

4 EMISSION SPECTRUM

We have subtracted the stellar population and verified that the effect in the final emission lines is small for Hα, but can be very important for Hβ, enhancing its intensity by a factor of 2 or more. This happens in the cases when the equivalent width of the emission line is small, of the order of the value for the underlying absorption (4 Å for a typical red stellar-population spectrum).

We have analysed the emission spectrum after subtraction of the template for the stellar population. We have measured the emission-line fluxes and full width at half maximum (FWHM) of the lines, which are shown in Tables 3, 5 and 7.

Table 3. Nuclear emission-line fluxes.

Line	N1667	N2992	N3281	N4388	N4507	N4939	N6890	I5063	I5135
3727	50.7	31.5	12.3	32.4	21.4	9.5	10.7	22.3	18.8
3869	22.3	6.5	-:	5.8	7.4	6.4	9.9	6.1	7.7
3970	-	-	-	0.7:	2.4	-	-	2.6	-
4101	-	1.6	-	1.7	3.1:	-	-	1.7	-
4340	-	5.3	-	4.5	5.4	4.7	-	4.6	4.9
4363	-	3.7	-	-	4.2	2.3	-	2.0	-
4686	-	2.5:	-	1.3:	0.9	2.0	-	1.6	-
4861	54.1	10.4	9.4	12.2	9.8	8.0	9.8	10.3	17.2
4959	42.1	29.8	35.4	34.0	31.3[1]	32.3	38.7	32.5	32.3
5007	100	100	100	100	100[1]	100	100	100	100
5198	20.9	-	3.7:	2.2:	-	-	-	2.0	4.1
5876	-	-	-	3.1	-	-	-	-	3.6:
6300	37.2	3.7:	-	8.4	5.3	-	-	5.7	8.9
6364	-	-	-	3.0	-	-	-	-	-
6548	74.3	10.1	24.8	9.7	5.5	16.4	11.4	6.3	21.2
6563	307.9	89.1[1]	66.9	53.1	54.9[1]	30.8	130.1[1]	79.3[1]	195.9[1]
6584	290.5	30.8	62.6	27.6	16.6	50.6	34.7	18.8	64.2
6717	115.5[3]	15.0	43.1[3]	16.8	8.5	5.1:	:	12.3	15.5
6731		12.2		14.7	6.8	10.3:	:	12.9	12.9
F(5007)[2]	66.84	1546.23	278.3	4213.2	1776.78	502.3	232.7	1752.0	396.4

[1]Sum of two components (see Table 4).
[2]Calibrated flux in units of 10^{-15} erg cm^{-2} s^{-1}.
[3]λ6717 + λ6731.

4.1 Broad components

In order to deblend Hα from [N II]$\lambda\lambda$6548, 6584, we have adjusted Gaussians to the profiles and verified that, for the galaxies NGC 2992, 4507, 6890, IC 5063 and 5135, a better adjustment is obtained if a broad Hα component is considered. Fig. 3(a)–(e) shows the comparison between the fit with and without a broad Hα component for these galaxies. In both cases, we have used the constraints that the FWHMs of $\lambda\lambda$6548, 6584 are identical and the intensity of λ6548 is 0.33 times that of λ6584. We have also detected broad components in [O III]$\lambda\lambda$4959, 5007 for NGC 4507, which are shifted 5 Å to the blue, shown in Fig. 4. The data relative to these line components are listed in Table 4.

4.2 Line widths

We have used the measured FWHM of the emission lines to investigate if they correlate with the critical density (N_{cr}) for collisional de-excitation of the forbidden lines and the ionization potential (De Robertis & Osterbrock 1984, 1986).

Table 4. Flux fractions, widths (km s^{-1}) and central wavelengths (Å) of line components.

Galaxy	Hα broad	Hα narrow	[OIII]λ5007 broad	[OIII]λ5007 narrow
N2992	.635	.365		
	1450	280		
	6562	6563		
N4507	.423	.577	.460	.540
	2070	400	1210	450
	6560	6563	5002	5007
N6890	.647	.353		
	2760	270		
	6568	6563		
IC5063	.565	.435		
	2320	430		
	6568	6563		
IC5135	.642	.358		
	1900	280		
	6568	6563		

First we have verified that most of the observed lines are broadened as compared to the instrumental profile (comparison-lamp lines), as can be seen in Fig. 5.

In order to use the blend [O II]$\lambda\lambda$3726, 3729, which we cannot resolve, we have simulated the resulting profile assuming several values for the FWHM of the individual lines for intensity ratios $I_1 = I_2$ and $I_1 = 2I_2$. The results are shown in Fig. 6, where we also show the single value proposed by De Robertis & Osterbrock (1.35). Intermediate-intensity ratios can be interpolated between the two curves. We point out that it is irrelevant for the ordinate values in Fig. 6 which line is designated I_1 or I_2. Consequently, all the possible ratios for densities in the range 10–10^4 (Osterbrock 1974) are contained between the limits shown in the figure. It can be seen that, for FWHM(blend) > 500 km s^{-1}, the correction factors are significantly lower than 1.35, regardless of the intensity ratio. These considerations imply that for NGC 2110, in De Robertis & Osterbrock's work, the corrections might be much smaller than that adopted by them, and consequently the [O II] lines would present a significant departure from the FWHM × log N_{cr} correlation. We have applied the correction obtained from Fig. 6 to the [O II]λ3727 blended profile in the cases in which its width was significantly broader than the instrumental value. For those limited by the instrumental width, we did not apply the correction.

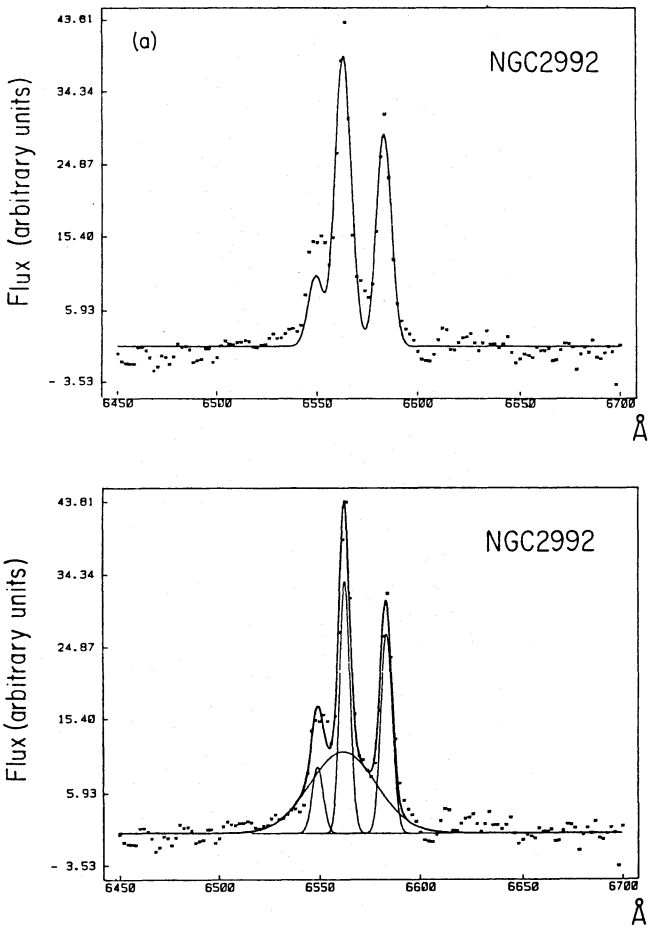

Figure 3. Comparison between the Gaussian fittings of the blend Hα + [N II] with and without a broad Hα component: thin line, individual components; thick line, total profile.

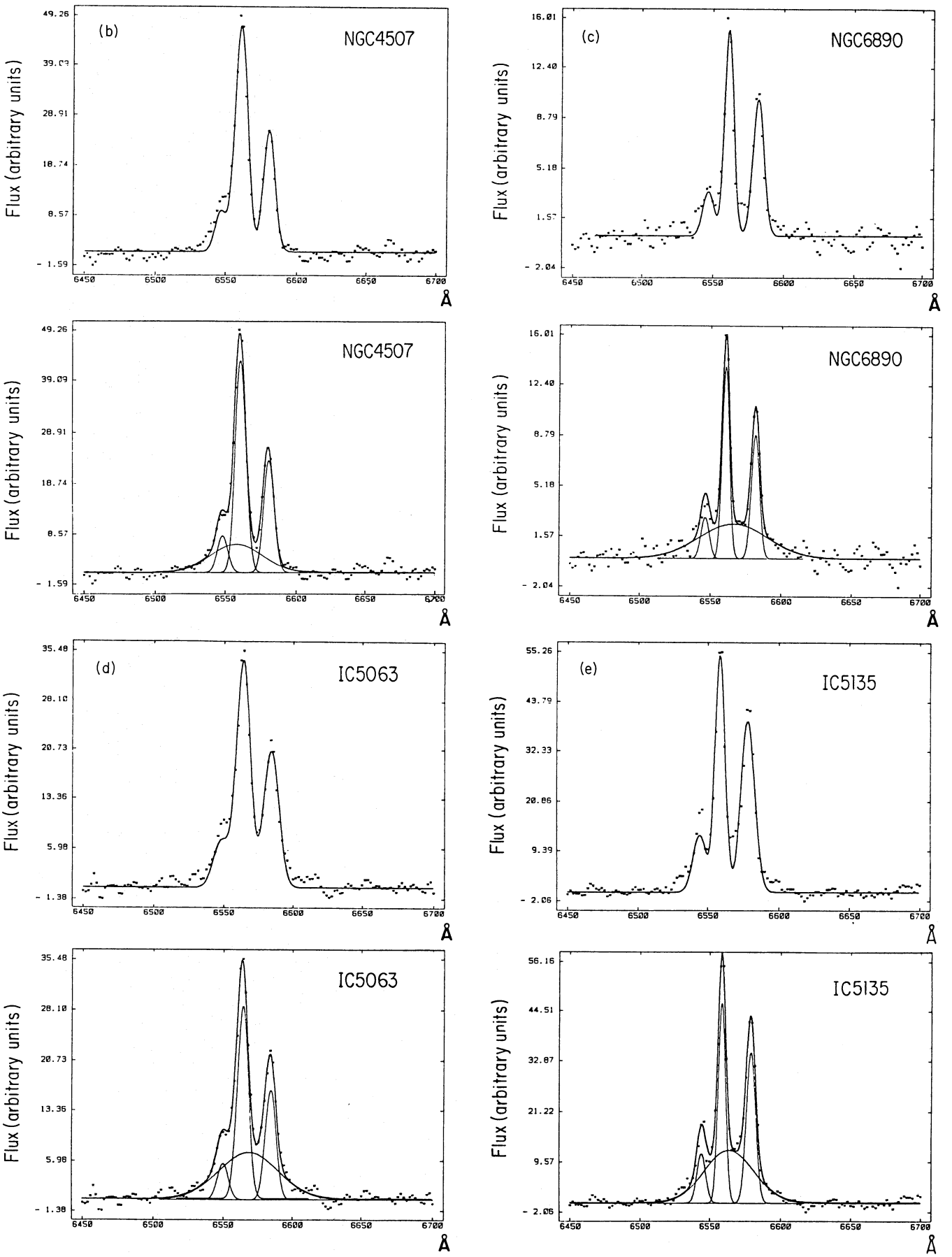

Figure 3 – *continued*

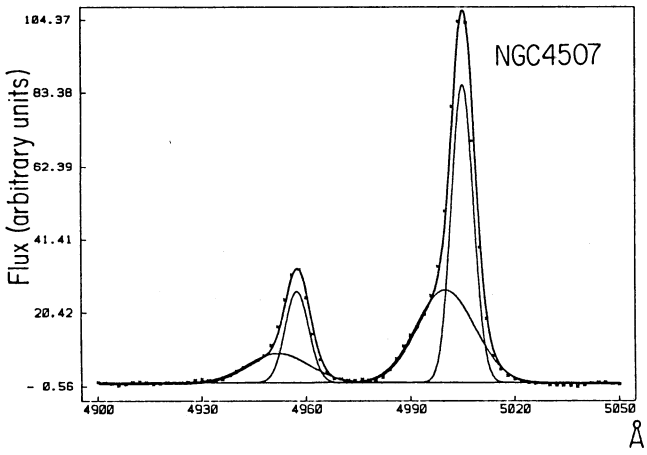

Figure 4. Fit of two Gaussian components to the [O III] λλ4959, 5007 profiles of NGC 4507; the broad component is displaced 5 Å to the blue.

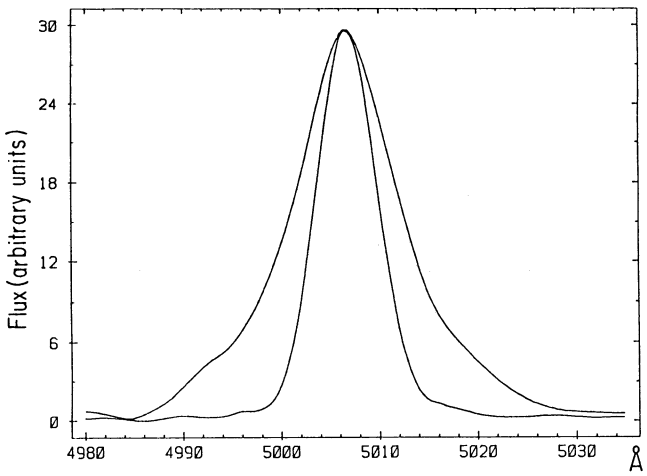

Figure 5. Comparison between the [O III] λ5007 profile and the instrumental one (narrower) for IC 5135.

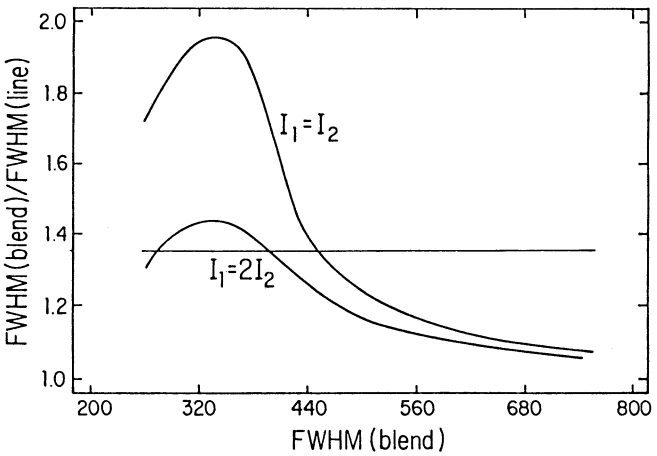

Figure 6. Ordinate: ratio between the FWHM of the blend [O II] λλ3726.0, 3728.8 and the FWHM of an unblended [O II] profile. Abscissa: FWHM of the blend for two representative relative peak intensities of the lines λ3726.0 and λ3728.8. Also shown as a straight line, the value adopted by De Robertis & Osterbrock (1986).

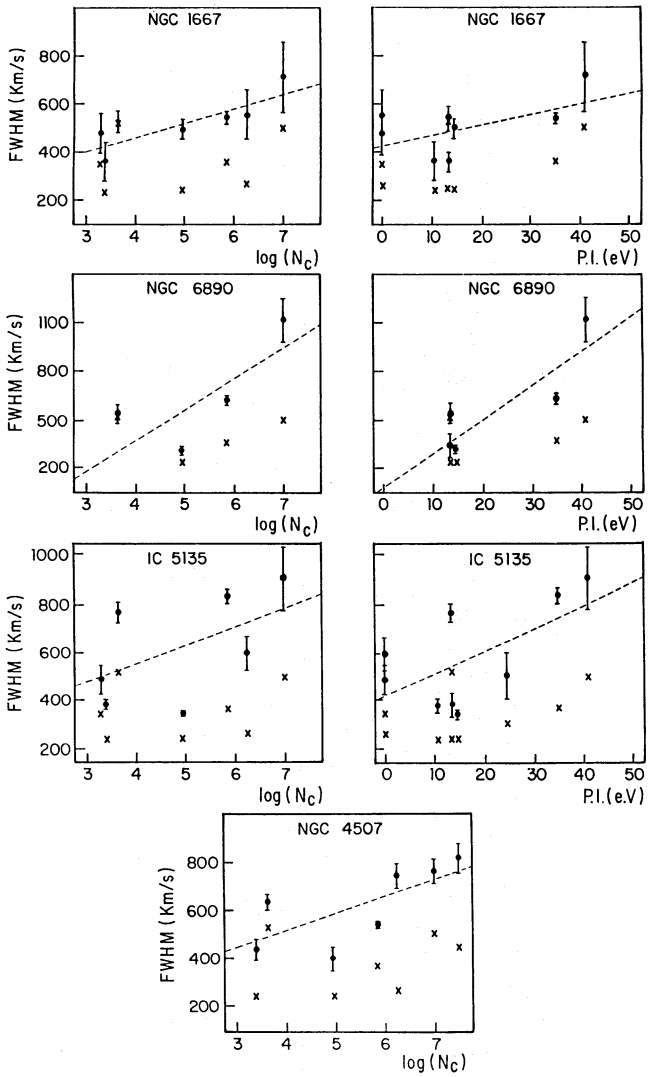

Figure 7. Correlations of emission-line widths (FWHM, Table 2) with logarithm of the critical density (forbidden lines) and with ionization potential (forbidden + permitted lines); observed values are plotted with error bars; crosses represent the instrumental value for each line. Dashed lines represent unweighted linear least-squares fits to the data.

We verified that the galaxies NGC 1667, 4507, 6890 and IC 5135 exhibit correlation between FWHM and N_{cr}, with a linear correlation coefficient $r > 0.6$. These galaxies, except NGC 4507, also exhibit a correlation between FWHM and ionization potential. In Fig. 7 we plot representative graphs showing these correlations. We preferred not to apply the usual corrections for intrinsic FWHM of each line as the square root of the difference between the squares of the observed and instrumental FWHMs. Rather we indicate in the figures the instrumental widths, so that the significance of the correlation can be directly judged from the limitations of the individual lines. The galaxies NGC 4939 and IC 5063 exhibit a weak correlation ($0.4 < r < 0.6$) between FWHM and N_{cr}. For NGC 2992, the FWHM correlates both with N_{cr} and ionization potential, but we consider this result marginal because the observed FWHMs for this galaxy are close to the instrumental limits.

The correlation between FWHM and N_{cr} for at least four and maybe in another three of the galaxies indicates the presence of clouds of different densities in the emitting gas and that the densest clouds have, on average, larger velocity dispersions (Fillipenko & Sargent 1988). The correlation of FWHM with ionization potential found for at least three of these galaxies indicates further that the densest clouds are the clouds where the highest ionization species are produced, probably due to the proximity of these clouds to the ionizing source. The same effect is observed in the nucleus of NGC 7469, for which a similar analysis was performed (Bonatto & Pastoriza 1990).

4.3 Physical parameters and chemical abundances

We have used the line fluxes which are shown in Table 3 for the nuclear spectra and in Table 5 for the off-nuclear ones to obtain physical parameters and elemental abundances for the emitting gas. We have used the ratio [S II] λ6717/λ6731 to calculate the gas density, whose values are shown in column 2 of Table 6. In column 3 we show the maximum acceptable range for the densities considering possible measurement errors in the [S II] ratio. When it was possible to detect the [O III] λ4363 line, we have used the ratio [O III] $\lambda\lambda$4959, 5007/λ4363 to calculate the electronic temperature (McCall 1984). These values are listed in column 4 for the densities obtained from [S II]. They are too high, when compared with those predicted by the photo-ionization models (see below) which best reproduce most of the observed emission-line ratios. This is due to the fact that the densities derived from the [S II] ratio cannot be applied to the [O III] lines: most of the [O III] lines, and mainly λ4363, are produced in clouds of larger density. As we have demonstrated from the correlation between FWHM and $\log(N_{cr})$, there is a range of densities in the emitting gas. The lines of higher N_{cr} are produced in the higher density clouds, with density values near N_{cr}. A clear discussion of this point can be found in Filippenko & Sargent (1988). We have thus checked the effect of a higher density in the calculus of the temperature. A reasonable value for the density of the clouds producing most of [O III] λ4363 is 10^6 cm^{-3}. We show in the last column of Table 6 the temperature values obtained for this higher density value, as well as the respective variations due to possible measurement errors in the line fluxes. We consider these last values a more realistic measurement of the temperature of the gas, and they agree with the values obtained from the photo-ionization models discussed below.

In the diagnostic diagrams of Baldwin, Phillips & Terlevich (1981), the observed galaxies occupy the locus of Seyfert 2 galaxies, except NGC 1667, which presents a smaller λ5007/Hβ ratio, more similar to the values presented by LINERS. As has been shown by Ferland & Netzer (1983), Halpern & Steiner (1983) and Terlevich & Melnick (1985), the emission-line ratios of Seyfert 2 and LINERS can be successfully reproduced by photo-ionization models when the ionizing source has a power-law spectrum due to a non-thermal ionizing source or to a blackbody of very high temperature. We have then compared our observed line ratios with photo-ionization model values in order to obtain more information about the ionizing continuum and emitting gas. We have used two models: the code CLOUDY (Ferland 1989; Ferland & Truran 1980; Ferland & Netzer 1983) for a constant-density nebula photo-ionized by a power-law spectrum; and the integrated model of Viegas-Aldrovandi & Gruenwald (1988), considering the contribution of clouds of different densities N_e following a distribution law $f(N_e) \propto N_e^{-b}$ for $10^2 < N_e < 10^6$ cm^{-3}, with a blackbody of 10^5 K as the ionizing source.

In Fig. 8(a)–(c), we show diagrams involving the strongest emission lines where we have plotted the data points and the model values which best reproduce them.

Table 5. Off-nuclear fluxes.

Line	N6890	IC5135
3727	-	119.0
4340	-	49.2
4861	174.4	185.7
5007	100	100.0
6548	:	184.1
6563	997.4	1017.5
6584	428.2	514.3
6717	-	149.2
6731	-	131.7
F(5007)[1]	9.075	24.97

[1] 10^{-15} erg cm^{-2} s^{-1}.

Table 6. Electronic densities N_e (cm^{-3}) and temperatures T (K).

Galaxy	Ne([SII])	Ne range	T(Ne[SII])	T(Ne=10⁴)
N2992	400	100[3] - 1200	21300	11300±1000
N4388	500[1]	300 - 800	-	-
N4507	400	100[3] - 1000	23000	11900± 800
N4939	15700	1400 - 100000[3]	15800	9300± 800
I5063	1000	400 - 2100	15200	9000± 600
I5135	400[1]	100[3] - 1400	-	-
north	400[2]	100[3] - 1600	-	-

[1] Assuming $T = 15\,000$ K.
[2] Assuming $T = 10\,000$ K.
[3] Density limits for the [S II] ratio.

Table 7. FWHM of emission lines in km s^{-1}.

Line	N1667	N2992	N3281	N4388	N4507	N4939	N6890	I5063	I5135
3727	520	610	514	698	685	637	492	762	850
3869	708	578	491	651	762	702	1109	645	902
3970	-	-	-	658:	736	-	-	699	-
4101	-	327	-	461	1162:	-	-	472	-
4340	-	826	-	531	849	893:	-	595	592
4363	-	763	-	-	819	550:	-	690	-
4686	-	744:	-	365:	381	447	-	537	-
4861	493	392	-	550	565	536	462	627	482
4959	776:	390	554	481	599	519	688	538	836
5007	542	399	449	465	539	472	624	513	834
5198	474	-	273:	765:	-	-	-	491:	489
5876	-	-	-	643	-	-	-	-	505:
6300	555:	259:	-	569	742	-	-	590	599
6364	-	-	-	563	-	-	-	-	-
6548[1]	365	313	381	426	393	385	313	415	344
6563	353	444	433	394	474	383	338	533	381
6584[1]	494	313	443	442	393	385	313	415	344
6717	360:	346	:	394	435	238:	:	441	382
6731	360:	312	:	394	435	339:	:	441	382

[1] [N II] lines are corrected for broad Hα whenever present.

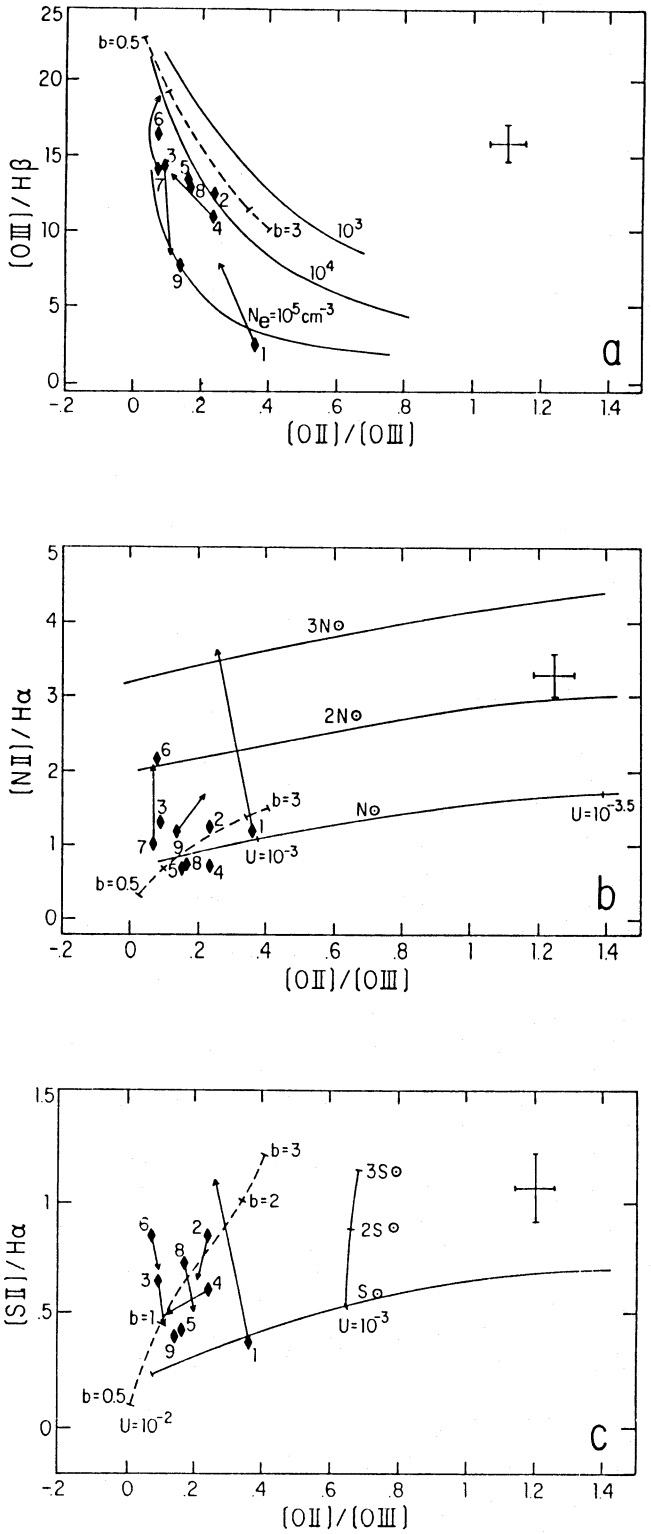

Figure 8. Observed emission-line ratios (numbers 1–9, Table 1) and photo-ionization model values (lines) which best reproduce them. Arrows show the displacement presented by some galaxies in the diagrams when a slit area from 3- to 6-times smaller is used. Continuous lines: Ferland (1989) photo-ionization models with $F_\nu \propto \nu^{-1.5}$. Dashed lines: integrated photo-ionization models considering the contribution of clouds with densities N following the distribution law $f(N) \propto N^{-b}$ for $10^2 < N < 10^6$ cm^{-3} (Viegas-Aldrovandi & Gruenwald 1988); for $b=0$ the high-density clouds dominate and for $b=3$ the lowest-density clouds dominate.

From Fig. 8(a) we conclude that the data are best reproduced by one-density models with $10^4 < N_e < 10^5$ cm^{-3}, photo-ionization parameter $10^{-3.5} < U < 10^{-2}$ and power-law spectrum $F_\nu \propto \nu^{-\alpha}$ with power-law index $\alpha = 1.5$. Other α indexes have been tried (Storchi Bergmann & Pastoriza 1989a,b), but $\alpha = 1.5$ is the value which better reproduces most of the emission-line ratios. The abundance is solar. Models with higher abundances give lower values for [O III], but we verified that models with twice the solar abundances can also reproduce the data if the density is enhanced by about a factor of five.

Fig. 8(b) indicates that both the single-density models and integrated models can reproduce the intensity of the [N II] λλ6548, 6584 lines. The model sequences presented are for $N_e = 10^4$ cm^{-3} and solar abundance, but we have verified that varying the density between 10^3 and 10^5 cm^{-3} will produce only a small horizontal displacement. In previous works (Storchi-Bergmann & Pastoriza 1989a,b) we also verified that the enhancement of the abundance of all the elements by a factor of 2 produces only a small vertical displacement and that the only way to obtain high [N II]/Hα ratios for Seyfert 2 nuclei is by enhancing the nitrogen abundance relative to the other heavy elements. We conclude that the observed data points can be reproduced by clouds with densities in the above-mentioned range and abundances between solar and twice solar. The only exception is the galaxy NGC 4939, whose [N II] value can only be reproduced if we enhance the nitrogen abundance by 2.5-times relative to the other heavy elements.

In Fig. 8(c), the vertical dispersion of the data can be well reproduced both by single-density models with $N_e = 10^3$ cm^{-3} by varying the sulphur abundance or by the integrated models by varying the relative contribution of the low-density clouds. Again, the effect of the enhancement of all the elements by a factor of 2 provides sequences very similar to that with solar abundance, and can also reproduce the data.

In order to verify the importance of the contamination of surrounding H II regions in our data, we have compared our emission-line ratios with those from previous observations using smaller apertures. For NGC 2992 we used the data of Durret & Bergeron (1988) who observed the galaxy with a slit of 2×6 arcsec^2; for NGC 4939 we used the data of Véron-Cetty & Véron (1986), for a slit of 4×4 arcsec^2; and for all the other galaxies we used the observations of Phillips *et al.* (1983), made with a slit of 2×4 arcsec^2. Our slit covers an area in the nuclear region from 3- to 6-times larger so we can verify the presence of more extended emission and check its nature. Also, we can have some clues on the kind of measurements one makes when observing with a small slit galaxies which are 3- to 6-times more distant.

In Fig. 8(a)–(c) we have indicated with an arrow the displacement from our values of the points corresponding to the smaller apertures. We only show the arrows when they are larger than the error bars. From Fig. 8(a), it can be seen that the more central spectrum shows higher excitation for the galaxies NGC 1667, 4388 and 6890. For NGC 3281 the central spectrum shows lower excitation. From Fig. 8(b), it can be seen that the [N II]/Hα value of NGC 1667 is enhanced by a factor of 3. For NGC 6890 the value is enhanced by a factor of 2. IC 5135 also presents a small enhancement in the [N II]/Hα ratio, as well as in the

[O II]/[O III] ratio. In Fig. 8(c), for most galaxies the nuclear data exhibit lower values for [S II], except for NGC 1667, for which the nuclear value is much higher.

We interpret the changes observed in the emission-line ratios as due to the presence of extended less excited ionized gas surrounding the nucleus, which was included in our slit. This gas is particularly evident in NGC 1667 and 6890, but was also detected in NGC 3281, 4388 and IC 5135. In the case of NGC 3281, the surrounding gas seems to have higher excitation than the nuclear gas. This contamination was not considered in the models, which can be safely used only to describe the more central data. Nevertheless, the conclusions obtained from Fig. 8(a) are not altered. In the case of Fig. 8(b), it can be seen that they are altered for two nuclei: the nuclear gas of NGC 1667 presents an abundance of nitrogen which is 3-times solar and of NGC 6890 2-times solar. In the case of Fig. 3(c), the comparison of our data to the more central ones leads us to interpret the lower nuclear [S II]/Hα values presented by the majority of the nuclei as due to the contribution of higher density clouds near the nucleus, except for NGC 1667. For this galaxy, which exhibits high [S II]/Hα in the nucleus, we favour the interpretation of sulphur overabundance 3-times solar in the nuclear gas, as is observed for the nitrogen.

We remark that in spectral observations of distant active nuclei one observes a large region, which includes not only the active nucleus but also its surroundings. We have shown that this can mask the emission-line ratios of the nucleus itself and lead to wrong conclusions about its physical parameters and chemical abundance.

We have also compared the emission ratios obtained for the off-nuclear spectra of NGC 6890 and IC 5135 with the theoretical sequences of Dopita & Evans (1986) for H II regions in the diagrams $\log(4959,\ 5007/6548,\ 6584)\times\log(3727\cdot3727/4861\cdot6731)$, $\log(5007/4861)\times\log(3727/5007)$ and $\log(3727/6584)\times\log(3727\cdot3727/4861\cdot6731)$. For NGC 6890 we conclude that the gas abundance is about 1.5-times solar, while for IC 5135 it is between 1.5- and 2-times solar, in agreement with the overall abundance of the nuclear gas.

5 CONCLUSIONS

We have studied the inner 2–5 kpc of nine Seyfert galaxies and verified that the typical stellar population is old with a metallicity from solar to twice solar. It doe snot differ from that of normal galaxies of the same morphological type, except for IC 5135, in which about 20 per cent of the flux at λ5870 Å is due to star-forming events in the last 10^8 yr. No non-stellar continuum is detected in the observed range. The effect of the subtraction of the stellar population is very important for Hβ. Broad Hα components (FWHM = 2000 km s^{-1}) were found for NGC 2992, 4507, 6890, IC 5063 and 5135. The correlation between FWHM and critical densities for NGC 4507, 1667, 6890 and IC 5135, indicates the presence of density stratification. The correlation between FWHM and ionization potential for the last three indicates further an ionization structure. The comparison of our observed ratios with published values obtained with smaller apertures indicates the presence of extended ionized gas surrounding the nucleus for most galaxies, probably due to neighbouring H II regions, which are evident in the off-nuclear spectra obtained for NGC 6890 and IC 5135. From the emission-line ratios and using photo-ionization models, we have found that the gas has densities in the range $10^3 < N_e < 10^6$ cm^{-3}, temperatures of about 10^4 K and is photo-ionized by a power-law spectrum $F_\nu \propto \nu^{-1.5}$. The chemical abundance ranges from solar to twice solar. In addition, we obtain a nitrogen overabundance for the nuclear gas in NGC 4939 and 6890, and of nitrogen and sulphur for NGC 1667. We have also shown that the contamination of the nuclear gas by surrounding emission can lead to wrong conclusions about its properties. Thus care must be taken in the study of the spectra of distant active galaxies where even small apertures represent large regions within the galaxy.

ACKNOWLEDGMENTS

We are grateful to the Cerro Tololo Inter-American Observatory, where the observations were made, in particular to S. Heathcothe, A. Phillips and M. Navarrete for assistance with the observations and reductions. We also thank an anonymous referee for valuable suggestions which improved the paper. This work was partially supported by the Brazilian institutions FINEP, CNPq and FAPERGS.

REFERENCES

Adney, K. J., Wilson, A. S. & Baldwin, J. A., 1984. *Astr. J.*, **89,** 1514.
Baldwin, J. A., Phillips, M. M. & Terlevich, R., 1981. *Publs astr. Soc. Pacif.*, **93,** 5.
Baldwin, J. A., Wilson, A. S. & Whittle, M., 1987. Preprint Steward Obs. No. 717.
Bergeron, J., Durret, F. & Boksenberg, A., 1983. *Astr. Astrophys.*, **127,** 322.
Bica, E., 1988. *Astr. Astrophys.*, **195,** 76.
Bica, E. & Alloin, D., 1986a. *Astr. Astrophys.*, **162,** 21.
Bica, E. & Alloin, D., 1986b. *Astr. Astrophys.*, **166,** 83.
Bonatto, C. J. & Pastoriza, M. G., 1990. *Astrophys. J.*, **353,** 445.
Colina, L., Fricke, K. J., Kollatschny, W. & Perryman, M. A. C., 1987. *Astr. Astrophys.*, **178,** 51.
De Robertis, M. M. & Osterbrock, D. E., 1984. *Astrophys. J.*, **286,** 171.
De Robertis, M. M. & Osterbrock, D. E., 1986. *Astrophys. J.*, **301,** 727.
Dopita, M. A. & Evans, I. N., 1986. *Astrophys. J.*, **307,** 431.
Dressler, A. & Sandage, A., 1978. *Publs astr. Soc. Pacif.*, **90,** 5.
Durret, F. & Bergeron, J., 1988. *Astr. Astrophys. Suppl.*, **75,** 273.
Ferland, G. J., 1989. *Internal Report 89-001,* Astronomy Department, Ohio State University.
Ferland, G. J. & Netzer, H., 1983. *Astrophys. J.*, **264,** 105.
Ferland, G. J. & Truran, J. W., 1980. *Astrophys. J.*, **244,** 1022.
Filippenko, A. V., 1985. *Astrophys. J.*, **289,** 475.
Filippenko, A. V. & Sargent, W. L. W., 1988. *Astrophys. J.*, **324,** 134.
Halpern, J. P. & Steiner, J. E., 1983. *Astrophys. J.*, **269,** L37.
Koski, A. T., 1978. *Astrophys. J.*, **233,** 56.
McCall, M. L., 1984. *Mon. Not. R. astr. Soc.*, **208,** 253.
Osmer, P. S., Smith, M. G. & Weedman, D. W., 1974. *Astrophys. J.*, **193,** 279.
Osterbrock, D. E., 1974. *Astrophysics of Gaseous Nebulae,* W. H. Freeman & Co., San Francisco.
Pelat, D., Alloin, D. & Fosbury, F. A. E., 1981. *Mon. Not. R. astr. Soc.*, **195,** 787.

Phillips, M. M., Charles, P. A. & Baldwin, J. A., 1983. *Astrophys. J.,* **266,** 485.

Sandage, A. & Tammann, G. A., 1981. *Revised Shapley–Ames Catalog of Bright Galaxies,* Carnegie Institute of Washington.

Schild, R. Tresch-Fienberg, X. & Huchra, J., 1985. *Astr. J.,* **90,** 441.

Shields, J. C. & Filippenko, A. V., 1988. *Active Galactic Nuclei, IAU Symp. No. 134,* p. 480, eds Osterbrock, D. E. & Miller, J. S., Kluwer, Dordrecht.

Sersic, J. L. & Pastoriza, M. G., 1967. *Mon. Not. R. astr. Soc.,* **79,** 152.

Storchi Bergmann, T. & Pastoriza, M. G., 1989a. *Astrophys. J.,* **347,** 195.

Storchi Bergmann, T. & Pastoriza, M. G., 1989b. *Proc. of the Elba Workshop on Chemical and Dynamical Evolution of Galaxies,* Elba, Italy, 1989.

Terlevich, R. & Melnick, J., 1985. *Mon. Not. R. astr. Soc.,* **213,** 841.

Véron-Cetty, M.-P. & Véron, P., 1986. *Astr. Astrophys. Suppl.,* **66,** 335.

Viegas-Aldrovandi, S. M. & Gruenwald, R. B., 1988. *Astrophys. J.,* **324,** 683.

Wilson, A. S., Baldwin, J. A., Sun, S. D. & Wright, A. F., 1986. *Astrophys. J.,* **310,** 121.